Aeroelastic characteristics of cylindrical hybrid composite panels with viscoelastic damping treatments

Won-Ho Shin[a], Il-Kwon Oh[b], Jae-Hung Han[a], In Lee[a],*

[a]*Division of Aerospace Engineering, Department of Mechanical Engineering, Korea Advanced Institute of Science and Technology, 373-1 Kusong-Dong, Yusong-Gu, Taejoin 305-701, Republic of Korea*
[b]*School of Mechanical Systems Engineering, Chonnam National University, 300 Yongbong-dong, Puk-gu, Gwang-Ju, 550-757, Republic of Korea*

Abstract

Supersonic flutter analysis of cylindrical composite panels with structural damping treatments has been performed using the finite element method based on the zig-zag layerwise shell theory. The natural frequencies and loss factors of cylindrical viscoelastic composites are computed considering the effects of transverse shear deformation. And Kumhaar's modified piston theory is applied for the calculation of aerodynamic forces. The flutter of cylindrical composite panels is analyzed considering structural damping effect. With respect to aeroelastic stabilities, various damping characteristics of unconstrained layer, constrained layer, and symmetrically co-cured sandwich laminates are compared with those of an original base panel.
© 2006 Elsevier Ltd. All rights reserved.

1. Introduction

Surface damping treatments may significantly improve acoustic and dynamic performance of flexible composite structures. Numerous studies [1,2] have been done on the damping mechanism and efficient damping treatments. The hybrid composite structures with co-cured, embedded and constrained damping layers have been applied in aerospace, automotive and electronic products. The embedded damping and constrained layers dissipate vibratory energy through improved transverse shear deformations. As a result, more accurate finite element models are required to describe the transverse shear mechanism, general ply orientation, thick cross-section, various boundary conditions and material degradation.

Among the previous works on the damping mechanics of composite structures, Saravanos and Pereira [3] developed a finite element based on the discrete layer laminate damping theory to predict the damped dynamic characteristics of composite plates with embedded damping layers, especially. Koo and Lee [4] developed the refined finite element model for describing the vibration and damping of anisotropic laminates in cylindrical

---

*Corresponding author. Fax: +82 42 869 3710.
E-mail addresses: swh@asdl.kaist.ac.kr (W.-H. Shin), ikoh@chonnam.ac.kr (I.-K. Oh), jaehunghan@kaist.ac.kr (J.-H. Han), inlee@asdl.kaist.ac.kr (I. Lee).

Nomenclature

		U^J, V^J	in-plane displacement at the Jth interface
		W	transverse displacement
f_i	body forces	β	aerodynamic pressure parameter
h	loss factor	γ	curvature term of Kurmhaar's piston theory
$\mathbf{M}$	mass matrix		
$\mathbf{q}$	out-of-balance vector	μ	aerodynamic damping parameter
Q_{ij}	elastic modulus	ρ	density of structures
$\overline{Q}_{ij}$	reduced elastic modulus ($\overline{Q} = R^{\mathrm{T}}QR$)	ρ_a	density of airflow
u_i	displacements	σ_{ij}	Cauchy stress tensor
$\mathbf{u}$	unknown displacement dof vector	$\overline{\psi}_k$	shape function

bending. Cho et al. [5] investigated the vibration and damping characteristics of laminated plates with fully and partially covered damping layers by applying the layerwise displacement plate theory. Lee and Kosmatka [6] suggested layerwise zig-zag theory for analysis of passively damped vibration of composite plates.

The literature survey revealed that a few papers were devoted to the investigation of the damping capacity of cylindrical composite shells with damping layers unlike flat composite plates. Ramesh and Ganesan [7] studied the harmonic response of cylindrical shells with constrained damping treatment. Baz and Chen [8] investigated the control method of axi-symmetric vibrations of cylindrical shells using active constrained layer damping. Lee et al. [9] investigated the dynamic characteristics of cylindrical composite panels with co-cured and constrained viscoelastic layers. In this paper, viscoelastic materials are examined according to environmental temperature and excitation frequencies with refined layerwise finite element mechanics to accurately describe the transverse shear deformation and sectional warping.

The external skins of high-speed aircrafts are exposed to severe aerodynamic flow and high or low environmental temperatures. In this case, an aeroelastic self-excited oscillation of the external skin is a critical problem known as panel flutter. The comprehensive review of the mathematical and physical mechanism of panel flutter has been performed by Dowell [10]. Supersonic panel flutter is a considerable aeroelastic behavior in the design of external structures of launch vehicles, supersonic fighters and military missiles. To investigate the effect of various dampings on the flutter boundary, several authors have treated supersonic flutter of viscoelastic plates and shells. Johns and Parks [11] reported that hysteretic structural damping destabilized flutter characteristics. Ellen [12] presented spatial derivative arguments to show that structural damping can stabilize flutter boundary. Oyibo [13] presented the effect of viscous models for both structural and aerodynamic damping and proved the dual nature of viscous damping stabilization and destabilization. Recently Koo and Hwang [14] investigated the dual mechanism of structural damping of composite plates. They reported that the effect of structural damping is dependent on the fiber orientation of the composite plates because the flutter mode can be weak or strong according to the fiber orientation.

Unlike flat panels, the research on the aeroelastic behavior of cylindrical structures has been very rare. Krumhaar [15] proposed a modified piston supersonic aerodynamic theory, which can be applied to cylindrical shells with a corrected term of the radius. Librescu wrote an excellent book [16] concerning the supersonic flutter of shell-type structures. As laminated composite materials were being used more frequently in the design of external skin of high-speed vehicles, supersonic flutter of composite panels received resurgent interest in the early 1990s. Bismarck-Nasr [17] investigated the aeroelasticity of laminated fiber reinforced shallow shells by using finite element method. Pidaparti and Yang [18] carried out supersonic flutter analysis of laminated composite plates and shells by using a doubly curved quadrilateral thin shell finite element based on the Kirchhoff–Love thin shell theory. Krause and Dinkler [19] investigated the influence of curvature and damping on flutter behavior. Bismarck-Nasr and Bones [20] studied damping effects in panel flutter for thin cylindrical shells, neglecting transverse shear effect.

There has been no published study on supersonic flutter characteristics of cylindrical composite panels with viscoelastic damping treatments. This paper attempts to investigate panel flutter characteristics of cylindrical hybrid composite shells with viscoelastic layers. To fully consider the effects of the structural damping, the transverse shear and the variable in-plane displacements through the thickness are accurately modeled. In this

study, we applied the discrete layer theory in the formulation of the finite element method, which was previously verified in our research of composite plates [21,22] and cylindrical panels [9,23]. This finite element model can give accurate results on the transverse shear deformations and loss factors for various damping treatments of cylindrical hybrid composite shells with viscoelastic layers.

2. Layerwise finite element formulations

2.1. Description of layerwise displacement fields

Based on the layerwise laminate theory [9,23], the displacement fields (u, v and w) on the $x - \phi - z$ coordinate system shown in Fig. 1 can be expressed by introducing the following piecewise continuous approximations. By introducing the piecewise interpolation function along thickness direction $\Phi^J(z)$ and finite element shape functions $\psi_I(\xi, \eta)$, the layerwise description is given as follows (Fig. 2):

$$u_1 = \sum_{J=1}^{NID} U^J(x, \phi, t)\Phi^J(z) = \sum_{J=1}^{NID}\sum_{I=1}^{NPE} U_I^J(x_I, \phi_I, t)\psi_I(\xi, \eta)\Phi^J(z),$$

$$u_2 = \sum_{J=1}^{NID} V^J(x, \phi, t)\Phi^J(z) = \sum_{J=1}^{NID}\sum_{I=1}^{NPE} V_I^J(x_I, \phi_I, t)\psi_I(\xi, \eta)\Phi^J(z),$$

$$u_3 = W(x, \phi, t) = \sum_{I=1}^{NPE} W_I(x_I, \phi_I, t)\psi_I(\xi, \eta), \tag{1}$$

where U_I^J and V_I^J are the in-plane displacements at the Ith node of the Jth interface; NID means the number of sub-lamina of the plates with degrees of freedom (dof). We applied the concept of sub-lamina of multi-layered structures with proper thickness discretization to reduce the computational time and the memory storage needed in the full layerwise mechanics. The NPE means the number of nodes per element. The linear
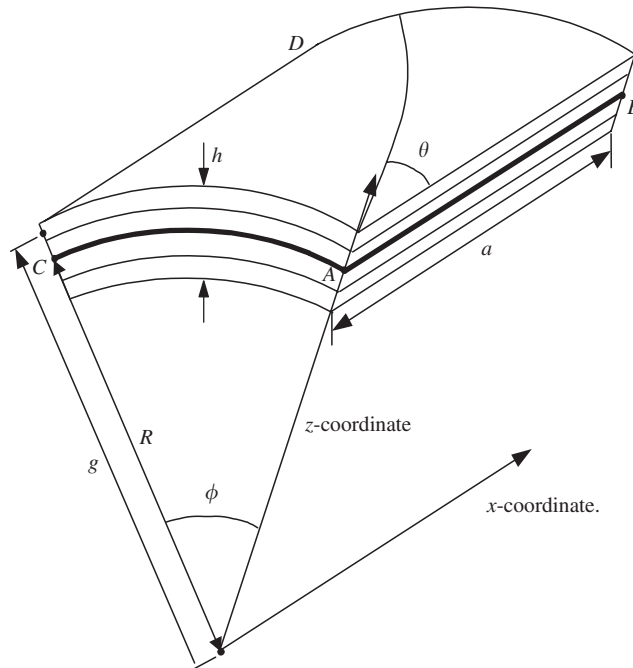

Fig. 1. Geometry of cylindrical composite panels and layerwise in-plane displacement.
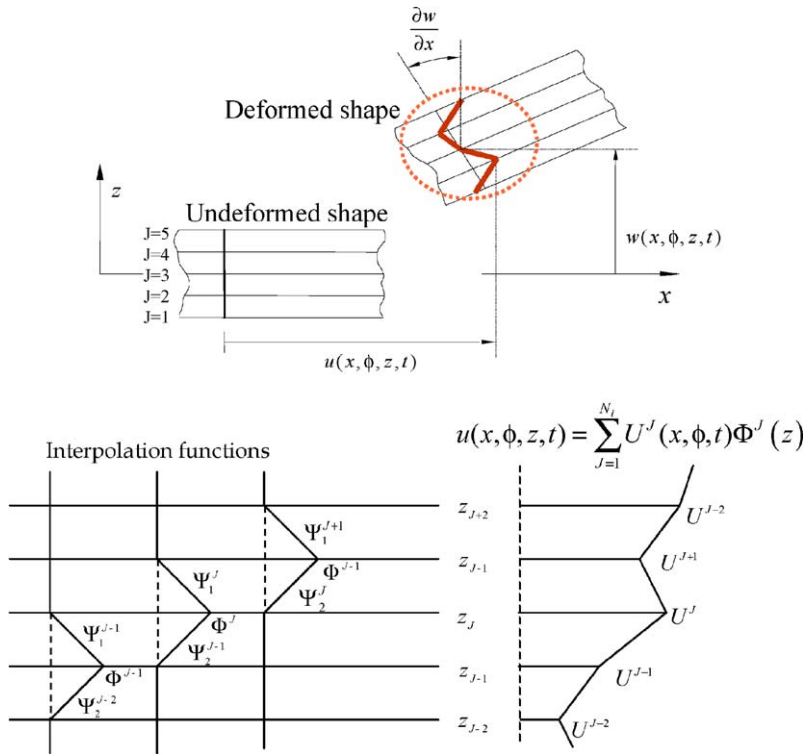
Fig. 2. Layerwise in-plane displacement and interpolation functions between layers of cylindrical panel.

relationships between strain and displacement can be written as follows:

$$
\varepsilon_{xx} = \frac{\partial u}{\partial x} = \sum_{J=1}^{N_i} \frac{\partial U^J}{\partial x} \Phi^J, \quad \varepsilon_{\phi\phi} = \frac{\partial v}{g\partial \phi} + \frac{w}{g} = \sum_{J=1}^{N_i} \frac{\partial V^J}{g\partial \phi} \Phi^J + \frac{W}{g},
$$

$$
\gamma_{x\phi} = \frac{\partial u}{g\partial \phi} + \frac{\partial v}{\partial x} = \sum_{J=1}^{N_i} \left(\frac{\partial U^J}{g\partial \phi} + \frac{\partial V^J}{\partial x} \right) \Phi^J, \quad \gamma_{xz} = \frac{\partial w}{\partial x} + \frac{\partial u}{\partial x} = \frac{\partial W}{\partial x} + \sum_{J=1}^{N_i} U^J \frac{d\Phi^J}{dz},
$$

$$
\gamma_{\phi z} = \frac{\partial w}{g\partial \phi} + \frac{\partial v}{\partial z} - \frac{v}{g} = \frac{\partial W}{g\partial \phi} + \sum_{J=1}^{N_i} V^J \frac{d\Phi^J}{dz} - \sum_{J=1}^{N_i} \left(\frac{V^J}{g} \right) \Phi^J. \tag{2}
$$

2.2. Constitutive equations of viscoelastic materials

Mechanical properties of layered composite and viscoelastic materials are generally defined by the complex modulus that is dependent on the excitation frequencies and the environmental temperature. Young's modulus and shear modulus can be expressed in the following form:

$$
\overline{E}_{II}(\omega, T) = E_{II}(\omega, T)(1 + i\eta_{II}(\omega, T)) \quad \text{for } I = 1, 2, 3, \tag{3}
$$

$$
\overline{G}_{12}(\omega, T) = G_{12}(\omega, T)(1 + i\eta_{12}(\omega, T)),
$$
$$
\overline{G}_{23}(\omega, T) = G_{23}(\omega, T)(1 + i\eta_{23}(\omega, T)),
$$
$$
\overline{G}_{13}(\omega, T) = G_{13}(\omega, T)(1 + i\eta_{13}(\omega, T)). \tag{4}
$$

In this study, all independent elastic and dissipative properties of the composite and viscoelastic plies are considered.

The linear constitutive equations for the kth lamina between sinusoidal stresses and strains with respect to the material coordinate can be written as

$$
\left\{
\begin{array}{c}
\sigma_1 \\
\sigma_2 \\
\sigma_3 \\
\sigma_{23} \\
\sigma_{13} \\
\sigma_{12}
\end{array}
\right\}_k
=
\begin{bmatrix}
Q_{11} & Q_{12} & Q_{13} & 0 & 0 & 0 \\
Q_{12} & Q_{22} & Q_{23} & 0 & 0 & 0 \\
Q_{13} & Q_{23} & Q_{33} & 0 & 0 & 0 \\
0 & 0 & 0 & Q_{44} & 0 & 0 \\
0 & 0 & 0 & 0 & Q_{55} & 0 \\
0 & 0 & 0 & 0 & 0 & Q_{66}
\end{bmatrix}_k
\left\{
\begin{array}{c}
\varepsilon_1 \\
\varepsilon_2 \\
\varepsilon_3 \\
\varepsilon_{23} \\
\varepsilon_{13} \\
\varepsilon_{12}
\end{array}
\right\}_k
\tag{5}
$$

and

$$
\begin{aligned}
&Q_{11} = (1 - v_{23}v_{32})\overline{E}_{11}/\Delta, \quad Q_{12} = (v_{12} + v_{13}v_{32})\overline{E}_{22}/\Delta, \quad Q_{13} = (v_{13} + v_{12}v_{23})\overline{E}_{33}/\Delta, \\
&Q_{23} = (v_{23} + v_{21}v_{13})\overline{E}_{33}/\Delta, \quad Q_{22} = (1 - v_{13}v_{31})\overline{E}_{22}/\Delta, \quad Q_{33} = (1 - v_{12}v_{21})\overline{E}_{33}/\Delta, \\
&Q_{44} = \overline{G}_{23}, \quad Q_{55} = \overline{G}_{13}, \quad Q_{66} = \overline{G}_{12}, \\
&\Delta = 1 - v_{12}v_{21} - v_{23}v_{32} - v_{13}v_{31} - 2v_{21}v_{32}v_{13}.
\end{aligned}
\tag{6}
$$

The corresponding constitutive relation for an anisotropic lamina in reference to the initial configuration $x - \phi - z$ can be obtained by the coordinate transformation with the fiber angle θ:

$$
\{\sigma\}_k^{x\phi z} = [\overline{Q}(\omega, T)]\{\varepsilon\}_k^{x\phi z} = [Q_R(\omega, T) + iQ_D(\omega, T)]\{\varepsilon\}_k^{x\phi z}.
\tag{7}
$$

2.3. Derivation of governing equations

To derive the governing equation of motion for the cylindrical composite panels with viscoelastic layers, Hamilton's variational principle was applied in the following form:

$$
\int_V \rho \ddot{u}_i \delta u_i \, dV + \int_V \sigma_{ij} \delta \varepsilon_{ij} \, dV = \int_V f_i \delta u_i \, dV + \int_S \tau_i \delta u_i \, dS.
\tag{8}
$$

Here, an infinitesimal volume of a cylinder is given as $dV = g(z) \, d\phi \, dx \, dz$. Over each finite element, the displacements are expressed as a linear combination of shape functions and nodal values in the following form:

$$
(W, U^J, V^J) = \sum_{I=1}^{\text{NPE}} (W_I, U_I^J, V_I^J)\psi_I(\xi, \eta).
\tag{9}
$$

Four shape functions through the thickness direction were used, and eight and nine node C^0 Lagrange elements were used in this analysis. Let us define the nodal displacement vector for an element i as

$$
\mathbf{u}_e = \{ \mathbf{u}^0 \quad \mathbf{u}^1 \quad \mathbf{v}^1 \quad \mathbf{u}^2 \quad \mathbf{v}^2 \quad \cdots \quad \mathbf{u}^{\text{NID}} \quad \mathbf{v}^{\text{NID}} \}^T
\tag{10}
$$

and

$$
\begin{aligned}
&\mathbf{u}^0 = \{ W_1 \quad W_2 \quad \cdots \quad W_{\text{NPE}} \}^T, \\
&\mathbf{u}^J = \{ U_1^J \quad U_2^J \quad \cdots \quad U_{\text{NPE}}^J \}^T, \quad J = 1, 2, \ldots, \text{NID}, \\
&\mathbf{v}^J = \{ V_1^J \quad V_2^J \quad \cdots \quad V_{\text{NPE}}^J \}^T, \quad J = 1, 2, \ldots, \text{NID}.
\end{aligned}
\tag{11}
$$

By using Hamilton's variational principle and finite elements, the governing finite element equation of motion for the cylindrical composite panel can be obtained in the following form:

$$
\mathbf{M}_e \ddot{\mathbf{u}}_e + (\mathbf{K}_{eR}(\omega, T) + i\mathbf{K}_{eD}(\omega, T))\mathbf{u}_e = \mathbf{F}_e(\omega).
\tag{12}
$$

The detailed elements of Eq. (12) can be found in our previous work [9]. Through the assembly procedure of finite elements, global finite element equations of cylindrical hybrid composite shells according to excitation frequency and temperature can be expressed as

$$\mathbf{M}\ddot{\mathbf{u}} + (\mathbf{K}(\omega, T) + i\mathbf{K}_D(\omega, T))\mathbf{u} = \mathbf{F}(\omega). \tag{13}$$

The eigensystem matrices can be written in the following form with proper frequency ω_0 and temperature T_0.

The natural frequencies and modal loss factors can be determined by using following eigenvalue equations of the general complex form:

$$(\mathbf{K}(\omega_0, T_0) + i\mathbf{K}_D(\omega_0, T_0) - \lambda_n^* \mathbf{M})\mathbf{u} = \mathbf{0}. \tag{14}$$

From Eq. (14), the natural frequencies and loss factors for each mode are defined by the real and imaginary parts of the complex eigenvalue λ_n^*:

$$\omega_n^2 = \text{Real}[\lambda_n^*], \quad \eta_n = \frac{\text{Imag}[\lambda_n^*]}{\text{Real}[\lambda_n^*]}. \tag{15}$$

2.4. Aeroelastic finite element formulation

Based on the Krumhaar's modified supersonic piston theory [15] considering the curvature effect of cylindrical structures, the aerodynamic stiffness and damping matrices can be derived by using the virtual work done by the aerodynamic load ΔP in the following form:

$$\begin{aligned}\Delta P &= -\frac{\rho_a U_\infty^2}{\sqrt{M^2 - 1}} \left\{ \frac{\partial w}{\partial x} + \frac{1}{Ma_\infty} \left(\frac{M^2 - 2}{M^2 - 1} \right) \frac{\partial w}{\partial t} - \frac{1}{2R\sqrt{M^2 - 1}} w \right\} \\ &= -\beta \frac{\partial w}{\partial x} - \mu \frac{\partial w}{\partial t} + \gamma w, \end{aligned} \tag{16}$$

where M is the Mach number, and U_∞ is the freestream speed. β, μ and γ are the aerodynamic pressure parameter, damping parameter and radius coefficient, respectively; w is the transverse deflection of the skin panel. Here, one can obtain the aerodynamic force vector with respect to finite element nodal displacements as follows:

$$\mathbf{F} = -\mu \mathbf{A}_\mu \dot{\mathbf{u}} - (\beta \mathbf{A}_\beta - \gamma \mathbf{A}_\gamma)\mathbf{u}. \tag{17}$$

Through the assembly procedure, the global aeroelastic finite element equation can be obtained as follows:

$$\mathbf{M}\ddot{\mathbf{u}} + \mu \mathbf{A}_\mu \dot{\mathbf{u}} + (\mathbf{K} + i\mathbf{K}_D + \beta \mathbf{A}_\beta - \gamma \mathbf{A}_\gamma)\mathbf{u} = \mathbf{0}. \tag{18}$$

The full system equations have a skew symmetric aerodynamic matrix that requires very large dof and computational cost. To reduce computational time and cost, the modal reduction is adopted to find a linear flutter speed in this study. The modal vectors are obtained by using the following eigenvalue equation:

$$(\mathbf{K} - \omega^2 \mathbf{M})\mathbf{\Theta} = \mathbf{0}. \tag{19}$$

Aerodynamic damping always stabilizes the flutter boundary. Also, to investigate the pure effect of structural damping on the aeroelastic characteristics of hybrid composite panels, the reduced flutter equation without the aerodynamic damping term is derived by using the modal approach in the following form:

$$(\mathbf{K}^*(\beta) - \Omega^2 \mathbf{M}^*)\mathbf{U}^* = \mathbf{0}, \tag{20}$$

where

$$\mathbf{M}^* = \mathbf{\Theta}^{\mathrm{T}} \mathbf{M} \mathbf{\Theta}, \tag{21}$$

$$\mathbf{K}^* = \mathbf{\Theta}^{\mathrm{T}} (\mathbf{K} + i\mathbf{K}_D + \beta \mathbf{A}_\beta - \gamma \mathbf{A}_\gamma)\mathbf{\Theta}. \tag{22}$$

To non-dimensionalize the analysis results, the non-dimensional parameters are introduced as follows:

$$\beta^* = \beta \frac{a^3}{D}, \quad \Omega_i^* = \Omega_i \sqrt{a^4 \frac{\rho c}{D}} \tag{23}$$

and

$$\Omega = \Omega_R (1 + ig).$$

where β^* and Ω^* are the non-dimensional dynamic pressure and complex frequency, respectively; g is a damping coefficient. a and h are axial length and thickness of skin panel, respectively; D is rigidity of panel as defined by $D = E_2 h^3$ for anisotropic material.

3. Results and discussions

3.1. Structural models of cylindrical composite panels with viscoelastic layers

Extensive efforts have been made to suppress the vibration of composite structures by using passive and constrained layer damping as well as active vibration control. However, there have been only few studies on the flutter characteristics of cylindrical composite shells considering structure damping in the viscoelastic layers and composite layers. Therefore, this paper examined the aeroelastic characteristics of cylindrical composite shells with viscoelastic layers by using the finite element method based on the layerwise shell theory considering transverse shear deformations.

The cylindrical composite panels with viscoelastic layers shown in Fig. 3 were used for the aeroelastic analysis. It consists of an original panel, viscoelastic cores, and constrained layers. Four edges of AB, CD, AC and BD are all clamped. The information of lamination and thickness of cylindrical composite cylindrical panels is given in Table 1.
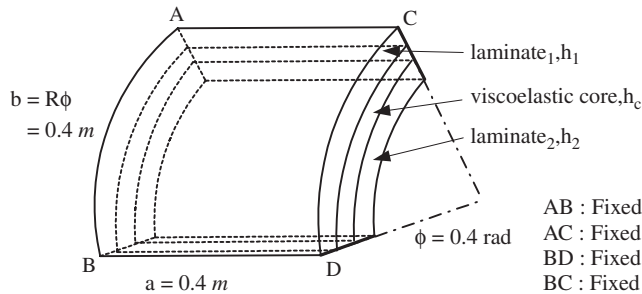
Fig. 3. Geometry and construction of cylindrical composite panels with viscoelastic layer.

Table 1
Lamination and thickness of cylindrical composite panels

	Laminate$_1$ (Gr/Ep)		Viscoelastic layer		Laminate$_2$ (Gr/Ep)	
	Lamination	Thickness (mm)	Isotropic	Thickness (mm)	Lamination	Thickness (mm)
Original panel	$[0_4/90_3]_s$	1.5	—	—	—	—
UCLD	$[0_4/90_3]_s$	1.5	[0]	0.25	—	—
CLD_$[90]_2$	$[0_4/90_3]_s$	1.5	[0]	0.25	$[90]_2$	0.25
CLD_$[0]_2$	$[0_4/90_3]_s$	1.5	[0]	0.25	$[0]_2$	0.25
Co-cured	$[0_4/90_3]$	0.75	[0]	0.25	$[0_4/90_3]$	0.75

CLD: constrained layer damping; UCLD: unconstrained layer damping; co-cured: embedded damping layer in center layer.

The composite material of lamina is graphite/epoxy, and material properties are given as follows:

$$E_1 = 119\,\text{GPa}, \quad E_2 = 8.67\,\text{GPa}, \quad G_{12} = G_{13} = 5.18\,\text{GPa}, \quad G_{23} = 3.9\,\text{GPa}, \quad v_{12} = 0.31,$$

$$\rho = 1570\,\text{kg/m}^3, \quad \eta_1 = 0.118\%, \quad \eta_2 = 0.620\%, \quad \eta_{12} = \eta_{13} = 0.812\%, \quad \eta_{23} = 0.846\%.$$

3M-ISD110 and 3M-ISD 112 were used as viscoelastic materials depending on the environmental temperature and the exciting frequency. The equations proposed by Drake [24] are given in the following equations:

$$\log_{10}(M) = \log_{10}(\text{ML}) + \frac{2\log_{10}(\text{MROM/ML})}{1 + (\text{FQROM/FR})^{\text{SLOPE}}}, \tag{24}$$

$$\log_{10}(\text{ETA}) = \log_{10}(\text{ETAFROL}) + \frac{C}{2}((\text{SH} + \text{SL})A + (\text{SL} - \text{SH})(1 - \sqrt{1 + A^2}). \tag{25}$$

Here, M (stiffness) and ETA (loss factor) are obtained from Eqs. (24) and (25), and are used to predict the material properties of 3M-ISD110 and 3M-ISD112. In this study, environmental temperature and frequency were assumed to be a constant.

3.2. Free vibration analysis

The 12×12 meshes with nine-node elements and four to six sub-laminates through the thickness direction were used as the layerwise finite element models. The original panel was a all-clamped 14-layered $[0_4/90_3]_s$ graphite–epoxy composite cylindrical panel of $400 \times 400 \times 1.75\,\text{mm}$. UCLD consists of the original panel and the ISD110 (or ISD 112) viscoelastic damping layer of $400 \times 400 \times 2.5\,\text{mm}$ located on lower face of the original panel. CLD is made up of the original panel, the viscoelastic layer, and the constrained layer located on the lower face of the original panel. $[0]_2$ and $[90]_2$ laminates were selected as the constrained layers. The co-cured sandwich model has an embedded viscoelastic layer in the center of the original panel.

Tables 2–4 show the natural frequencies, loss factors, and mode shapes for the original panel, UCLD, CLD, and the co-cured sandwich model according to viscoelastic material. When ISD 110 is used as the viscoelastic layers, the mode shapes of UCLD are similar to those of the original panel. The natural frequencies of UCLD decrease and the loss factors increase slightly due to the effect of the viscoelastic layer since the viscoelastic layer has high loss factor, but its modulus is negligibly small in comparison with that of graphite/epoxy layers. When CLD using $[0]_2$ plies as the constrained layer, the natural frequencies of longitudinal modes increase and the loss factors also increase remarkably. With regards to CLD using $[90]_2$ plies as the constrained layer, the
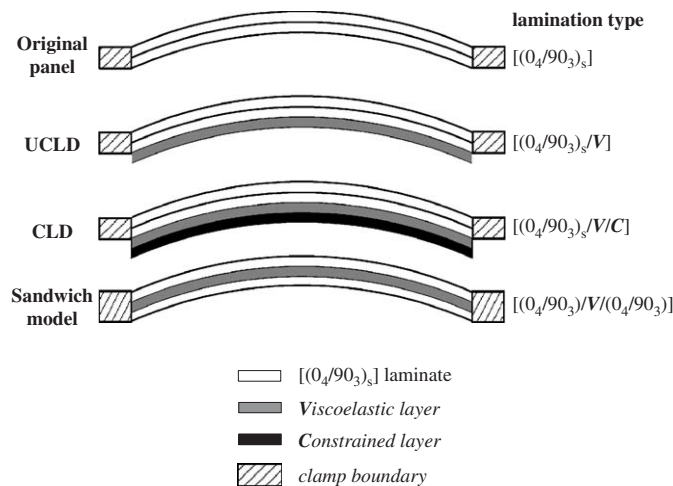
Fig. 4. Boundary conditions of hybrid panels for various damping treatments.

natural frequencies of circumferential modes increase and the loss factors increase considerably. When the co-cure sandwich model is used, the natural frequencies decrease but the loss factors increase dramatically.

The CLD and the co-cure sandwich models are better than the UCLD simply attaching the viscoelastic layer in view of the damping capacity. The co-cure sandwich model shows the highest damping capacity. This result shows that the case with viscoelastic layer attachment compared to the original panel with no viscoelastic layer attachment, the case using the constrained layers rather than the case with simply the viscoelastic layer attachment, and the condition of fastened constrained layers than that of loose constrained layer showed better damping efficiency. The co-cure sandwich model has a good damping efficiency, but it decreases the natural frequencies. So, it may be the good choice to select CLD considering the natural frequencies and damping efficiency. When ISD 112 is used as viscoelastic layers, t free vibration analysis tends to be similar that when ISD 110 is used (Fig. 4).
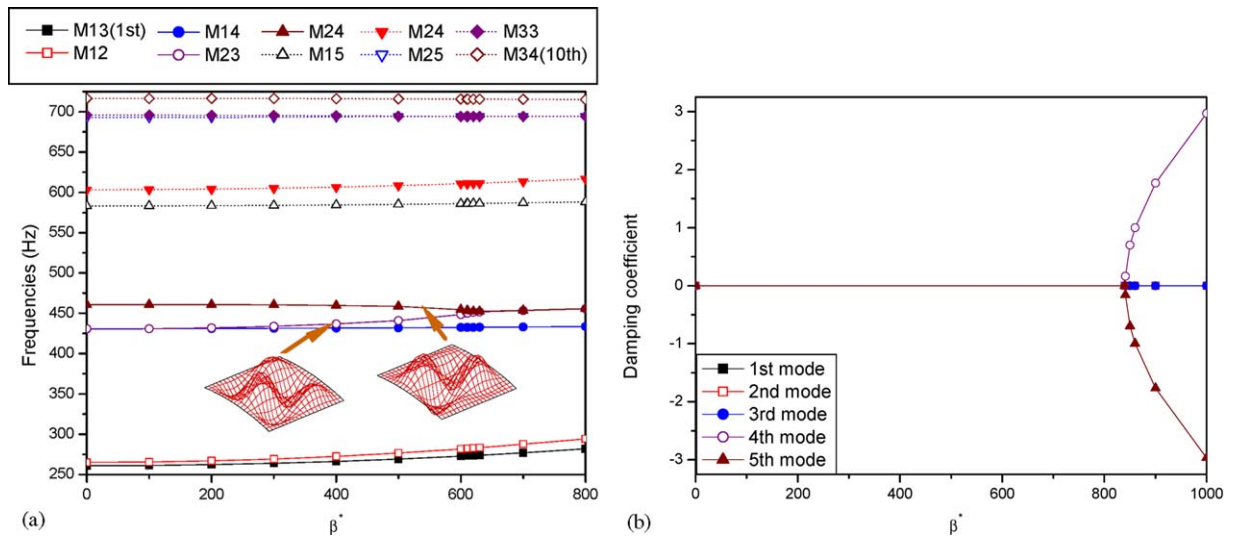
Fig. 5. Flutter history of cylindrical composite panel neglecting structural damping.
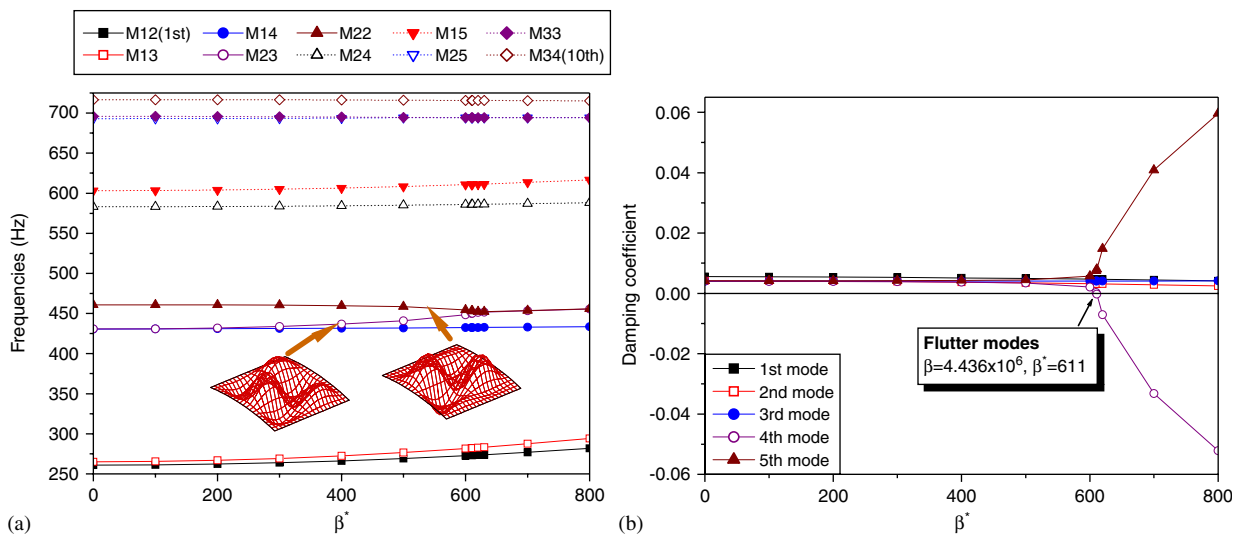
Fig. 6. Flutter history of cylindrical composite panel considering structural damping.

3.3. Aeroelastic effect of structural damping for cylindrical composite panel

Generally, structural damping is often neglected in flutter analysis. In previous studies [11–14] considering structural damping of a composite panel, total structural damping was simply assumed as g. However, structural damping has a significant effect on the dynamic and aeroelastic characteristics of vehicles or structures. So, in this study, structural damping was considered a type of loss factor, η, and was applied to not only the viscoelastic layer but also to each layer consisting of cylindrical composite panels. And then, the panel flutter analysis was performed by solving complex eigenvalue problems. Thirty normal modes were used in flutter analysis. The previous model used in free vibration analysis was also used in the panel flutter analysis. To calculate the aerodynamic force, Krumhaar's modified supersonic piston theory is applied.

The aeroelastic results of the original base composite panel neglecting structural damping are compared with those considering structural damping. Structural damping means the loss factor of graphite/epoxy layer consisting of the cylindrical composite panel. Panel flutter occurs at a point where the damping coefficients are lower than zero. As shown in Figs. 5 and 6, the two cases are very different.

When structural damping is neglected, the panel flutter occurs at dynamic pressure $\beta^* = 841$, when the two modes merge between fourth and fifth mode. The panel flutter also occurs between the fourth and fifth modes when structural damping is considered, but the flutter boundary changes remarkably. The flutter boundary (β^*) considering structural damping is reduced by 210, compared with that of the other.

The eigensolution of Eq. (18) has been represented as a complex form ($\lambda = \lambda_R + \lambda_I$) without a structural damping. The complex eigensolution λ have been obtained with real values ($\lambda_I = 0$) before a panel flutter occurs. Until the flutter point, real parts λ_R of eigenvalues of two flutter modes have got close to each other as aerodynamic pressure increases. At the flutter point, the frequency coalescence of two modes has happened and the eigensolution has been the conjugate complex.

With a structural damping ($K_D \neq 0$), the eigensolution λ have been complex values according to all aerodynamic pressure. Until the flutter point, real parts λ_R of two flutter modes also have got close to each other but do not merged as aerodynamic pressure increases. These eigensolutions with a damping gradually approach to the ones without a structural damping, which are asymptotic lines. The flutter with a structural damping occurs when the sign of the imaginary part λ_I changes to the negative value. The spread point, where the gap of the imaginary values between conjugate complex eigenvalue gets wide after mode coalescence, has located prior to the one without a structural damping. And the sign of imaginary parts changes the negative value before the flutter limit without a structural damping. Then the critical aerodynamic pressure of the aeroelastic systems considering the structural damping may be located prior to the one without a structural damping. Hence, it causes a decrease of the flutter boundary.
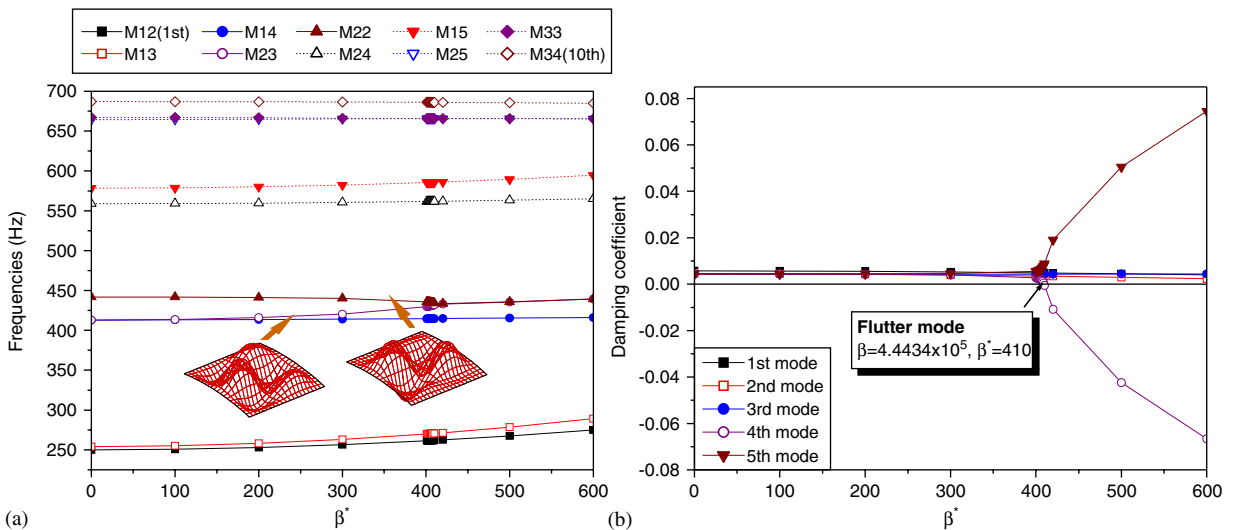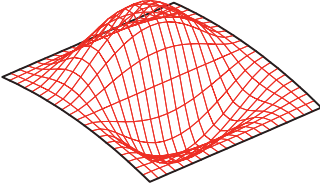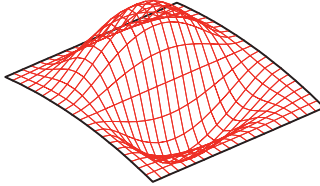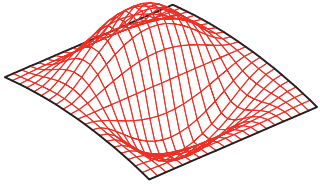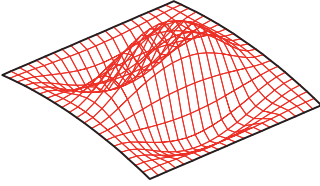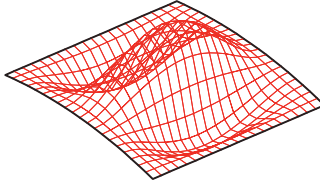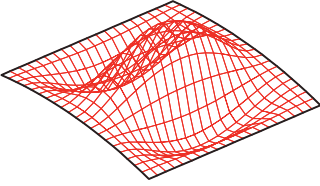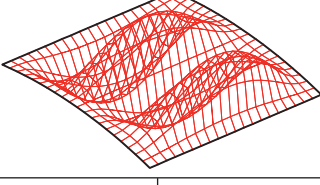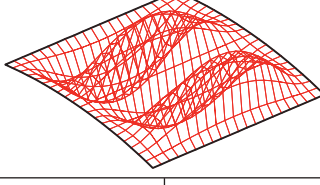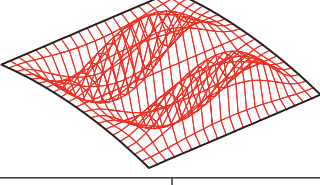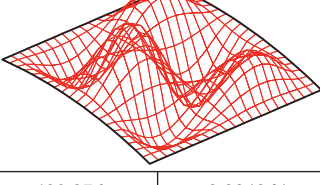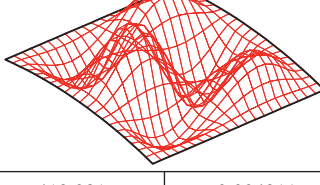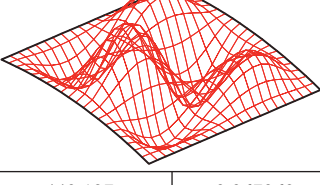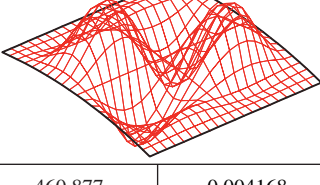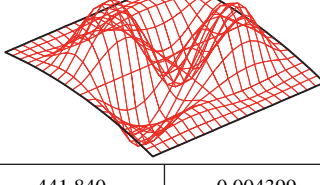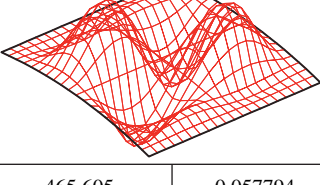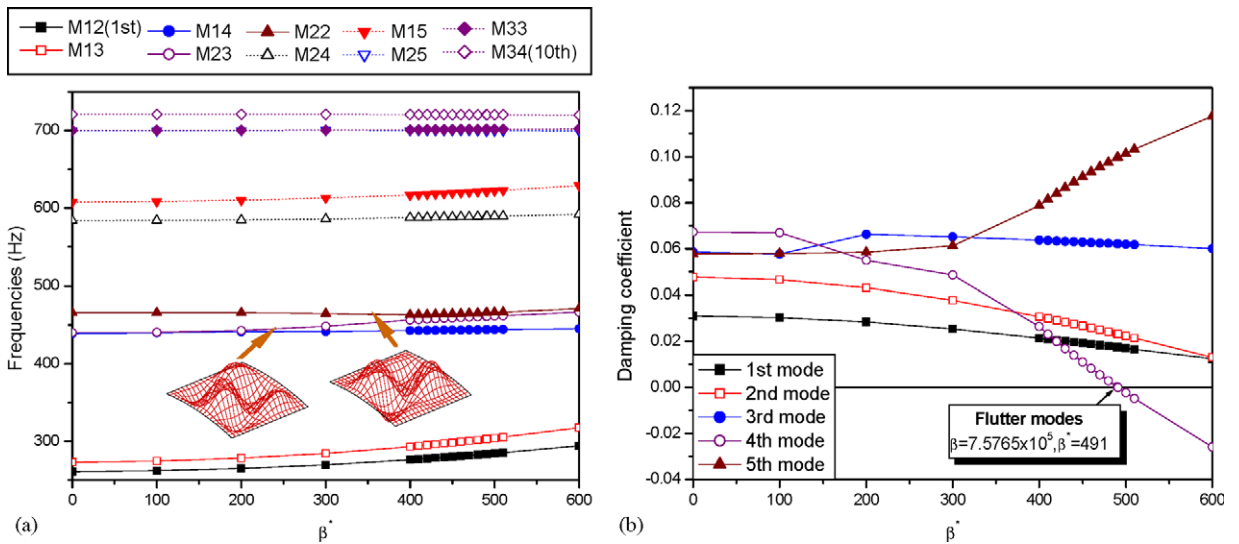

Fig. 7. Flutter history of UCLD with ISD 110 viscoelastic layer.

The results of this analysis are remarkable. It was thought that structural damping significantly affects aeroelastic characteristics. The loss factor of graphite/epoxy is often neglected in dynamic and aeroelastic analysis because it is very small ($\approx 10^{-3}$) compared to other material properties. In free vibration analysis
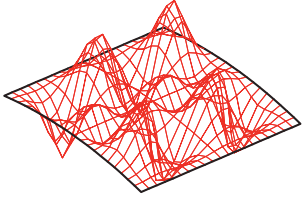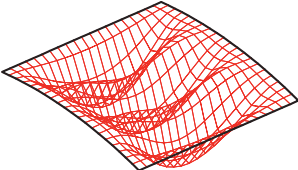
Table 2
Effect of damping treatments using ISD 110 as viscoelastic material on the flutter of cylindrical panel (I)

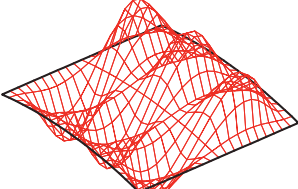| Modes	Original Panel ($[0_4/90_3]_s$)		UCLD ($[(0_4/90_3)_s/d]$)		CLD_$[0]_2$ ($[(0_4/90_3)_s/d/0_2]$)	
	Freq (Hz)	η	Freq (Hz)	η	Freq (Hz)	η
1st						
	260.875	0.005520	250.100	0.005736	261.044	0.030975
2nd						
	265.088	0.004184	254.154	0.004544	273.208	0.047776
3rd						
	430.575	0.003975	412.820	0.004384	438.736	0.58606
4th						
	430.876	0.004064	413.081	0.004311	440.127	0.067262
5th						
	460.877	0.004168	441.840	0.004399	465.605	0.057794
Flutter	4th & 5th	$\beta^* = 611$	4th & 5th	$\beta^* = 410$	4th	$\beta^* = 491$

considering the loss factor of graphite/epoxy, the loss factor of graphite/epoxy may be neglected because the difference between results with structural damping and results without structural damping is very small. But aeroelastic results show that structural damping significantly affects aeroelastic analysis although very slightly. Hence, it is very important to consider structural damping to accurately estimate the flutter boundary to achieve conservative aeroelastic design.

3.4. Flutter boundary of hybrid panels with damping treatments

Four cases are considered as damping treatments. The flutter characteristics of original base composite panel are compared with those of CLD (constrained layers damping treatment), UCLD (unconstrained layers damping treatment) and composite panel with embedded damping layer.

Firstly, in the case where ISD 110 is used as viscoelastic materials, as shown in Fig. 7 and Table 2, the flutter of UCLD model exists between the fourth and fifth modes. And the critical aerodynamic pressure β^* decreases by 201, compared with that of original base composite panel. As mentioned in the free vibration analysis, the density of a viscoelastic material is about twice that of a graphite/epoxy material, but the modulus of a

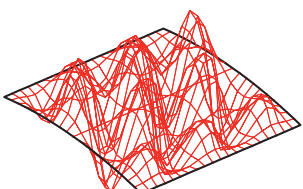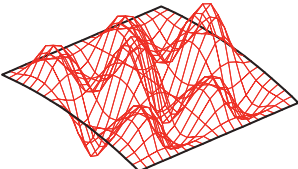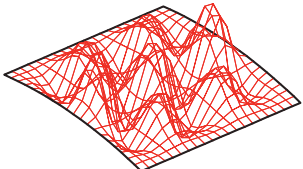Fig. 8. Flutter history of CLD_$[0]_2$ with ISD 110 viscoelastic layer.
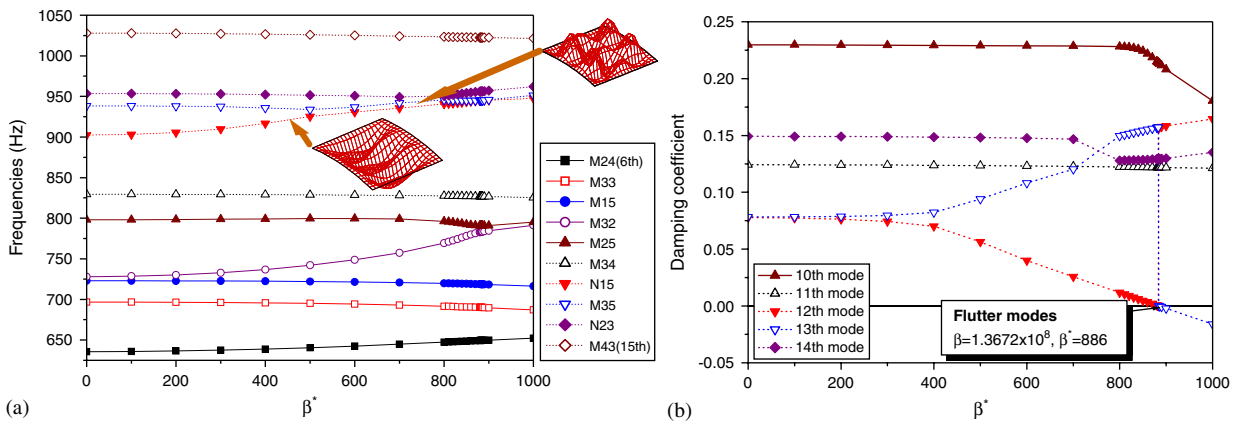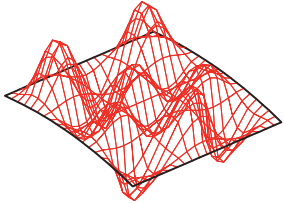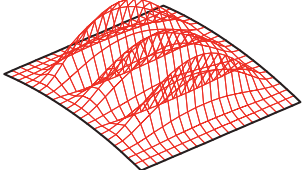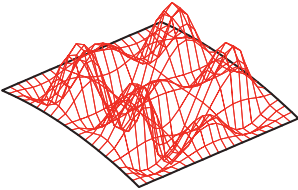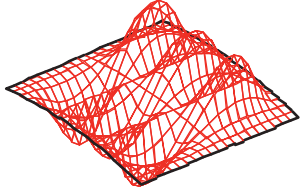
Fig. 9. Flutter history of CLD_$[90]_2$ with ISD 110 viscoelastic layer.

Table 3
Effect of damping treatments using ISD 110 as viscoelastic material on the flutter of cylindrical panel (II)

Modes	CLD_[90]$_2$ ([(0$_4$/90$_3$)$_s$/d/90$_2$])		Modes	Sandwich model ([0$_4$/90$_3$/d/0$_4$/90$_3$])	
	Freq (Hz)	η		Freq (Hz)	η
11th			19th		
	829.429	0.124250		829.734	0.304032
12th			20th		
	902.395	0.077656		849.824	0.0066873
13th			21st		
	938.248	0.078394		874.894	0.078057
14th			22nd		
	953.633	0.149155		910.799	0.454918
15th			23rd		
	1027.917	0.044842		910.736	0.434698
Flutter	13th	$\beta^* = 886$	Flutter	21st	$\beta^* = 656$

viscoelastic layer is much smaller than that of a graphite/epoxy layer. So, the natural frequencies of UCLD are less than those of the original base panel, and this affects the flutter boundary. Finally, the low frequency reduces the aeroelastic stability in view of non-dimensional aerodynamic pressures.

Figs. 8 and 9 and Tables 2 and 3 indicate the flutter boundaries in the cases of CLD_[0]$_2$ and CLD_[90]$_2$. When CLD_[0]$_2$ is used, flutter also occurs at the fourth mode. The constrained layers, [0]$_2$ plies, improve the longitudinal stiffness and increase the natural frequencies, but the panel flutter of the original model depends on the circumferential (φ-directional) mode mainly. So, [0]$_2$ layers provides the better aeroelastic stability than UCLD, but it does not improve the flutter boundary. The flutter boundary of CLD_[0]$_2$ decreases by 120, in compared with the flutter limit of original base composite panel. In free vibration analysis, CLD_[0]$_2$ shows the higher natural frequencies and the better loss factors than those of base panel. But CLD_[0]$_2$ has the lower flutter boundary than the original panel.

In the case of CLD_[90]$_2$, the aeroelastic unstable phenomenon is observed in higher mode than those in the cases of UCLD and CLD_[0]$_2$. The panel flutter occurs at the 13th mode. [90]$_2$ layers improve the circumferential stiffness, and it causes the improvement of the aeroelastic stability. The flutter boundary of CLD_[90]$_2$ increases by 275, compared with that of original base composite panel. CLD_[90]$_2$ shows improved results in free vibration as well as aeroelastic analysis.

As shown in Fig. 10 and Table 3, in the case of the model with an embedded damping layer, the panel flutter is observed in the higher mode than the instance of CLD_[90]$_2$ (comparison is not clear). It occurs at the 21st
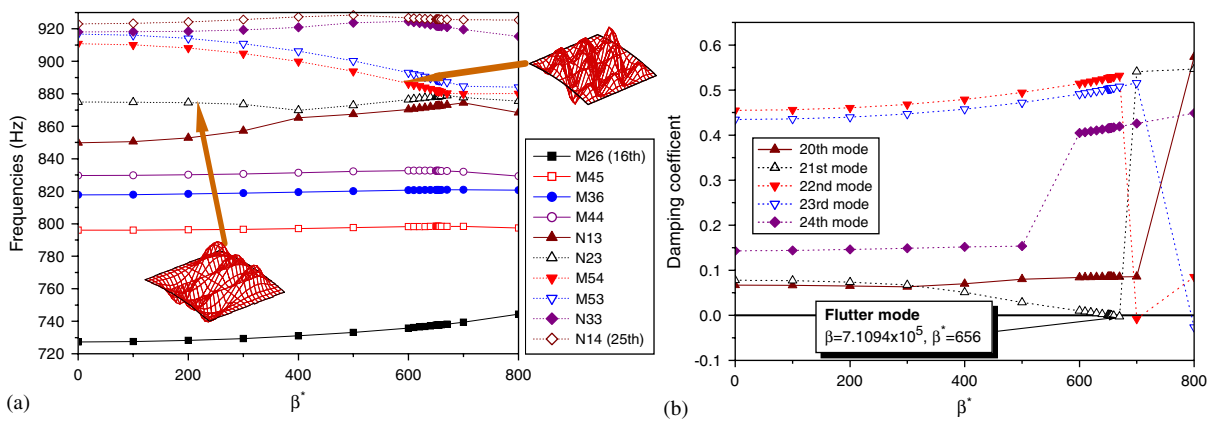

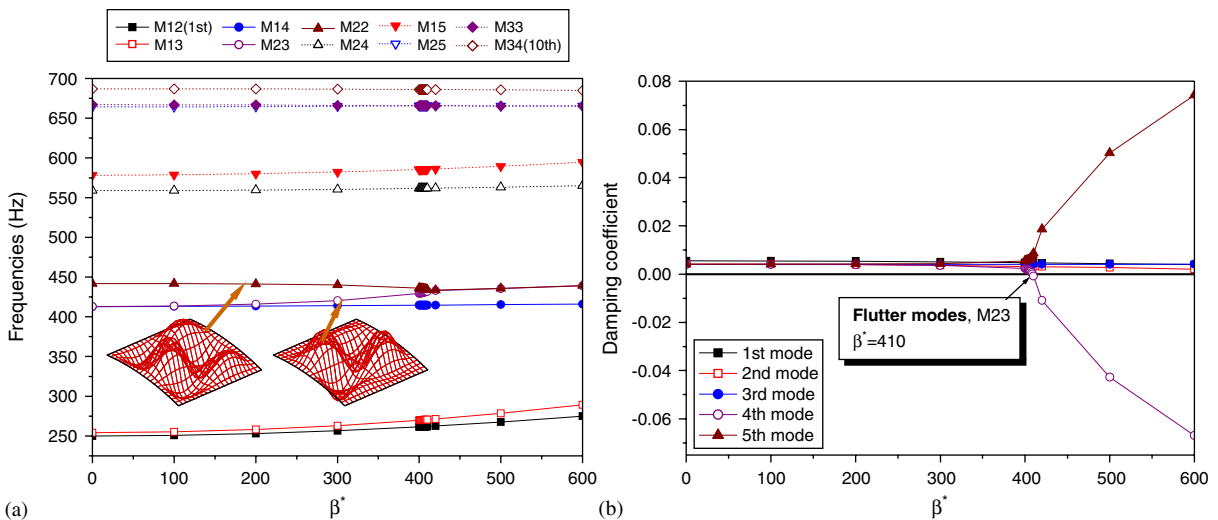Fig. 10. Flutter history of panel with embedded ISD 110 viscoelastic layer,
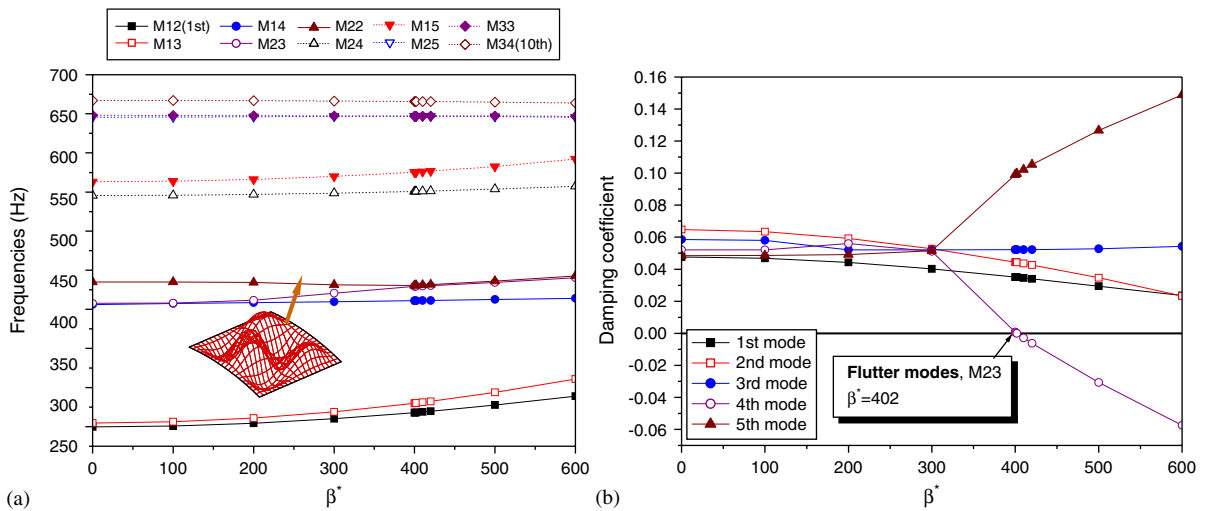

Fig. 11. Flutter history of UCLD with ISD 112 viscoelastic layer.

mode and the flutter boundary (β^*) increases by 45, compared with that of original base composite panel. The composite panel with embedded damping layer has the better aeroelastic stability and the better loss factor, but lower natural frequencies than the original base panel.

Secondly, in the case of using ISD 112 as viscoelastic materials, as shown in Fig. 11, the flutter of UCLD model has been observed between fourth and fifth modes. And the dynamic pressure β^* decreases by 201, compared with that of original base composite panel, resulting in the same value to the case using ISD 110. This result means that the viscoelastic layer does not affect to the aeroelastic stability for free boundary layer models.

Figs. 12 and 13 and Table 4 indicate the flutter boundaries for the cases of CLD_[0]$_2$ and CLD_[90]$_2$. In instance of CLD_[0]$_2$, the flutter also occurs between fourth and fifth modes. Similarly to the case using ISD 112, [0]$_2$ plies give better aeroelastic stability than UCLD, but it does not improve the flutter boundary in the view of non-dimensional flutter limit. The flutter boundary of CLD_[0]$_2$ decreases by 209, when compared with that of the original base composite panel. It has the lower flutter boundary than CLD_[0]$_2$ and UCLD using ISD 110.

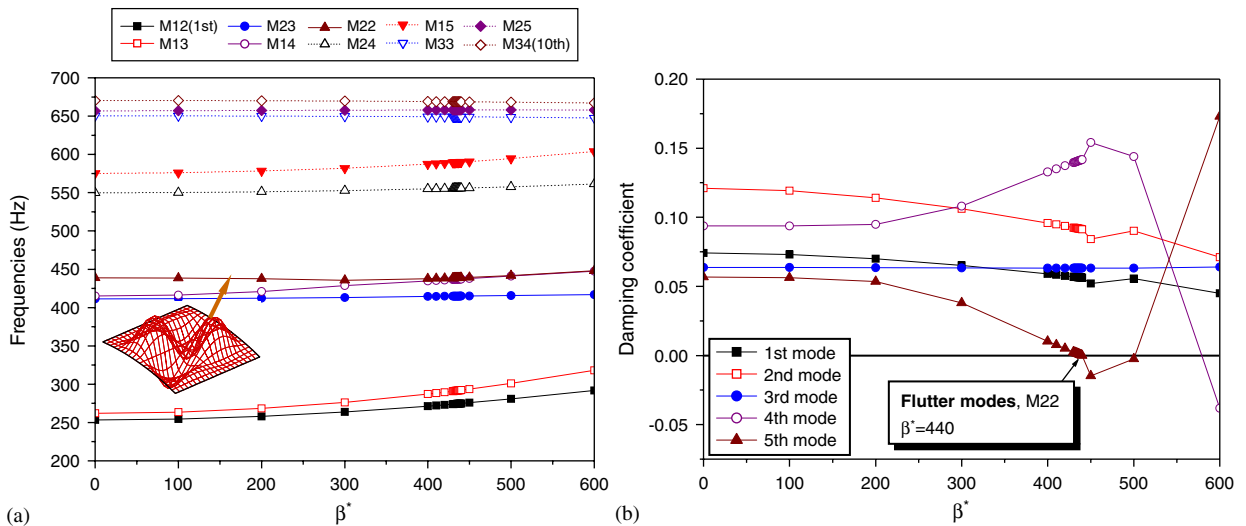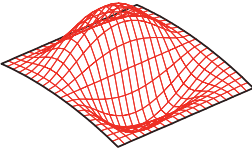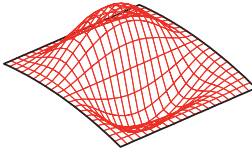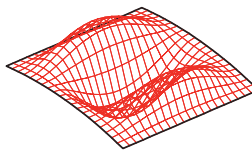Fig. 12. Flutter history of CLD_[0]$_2$ with ISD 112 viscoelastic layer.
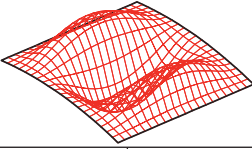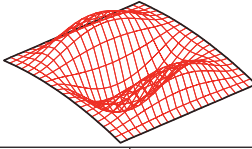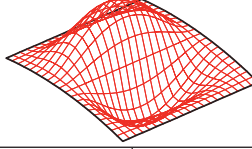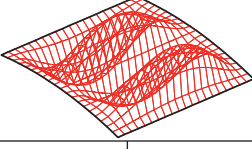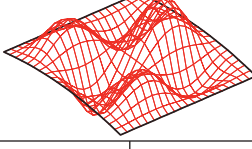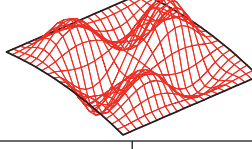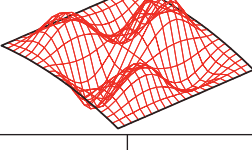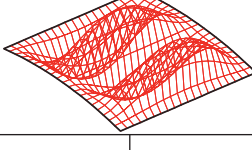
Fig. 13. Flutter history of CLD_[90]$_2$ with ISD 112 viscoelastic layer.

Table 4
Effect of damping treatments using ISD 112 as viscoelastic material on the flutter of cylindrical panel

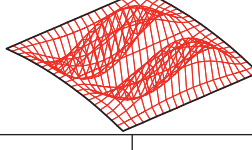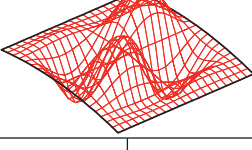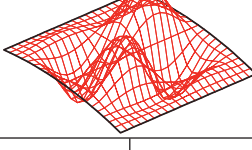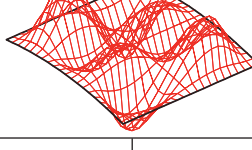| Modes	CLD_$[0]_2$		CLD_$[90]_2$		Sandwich model	
	Freq (Hz)	η	Freq (Hz)	η	Freq (Hz)	η
1st	249.726	0.047696	253.534	0.074186	182.373	0.128329
2nd	254.544	0.064809	262.047	0.121067	204.735	0.095230
3rd	406.046	0.058561	411.461	0.063768	280.126	0.116193
4th	407.724	0.052120	415.049	0.093783	289.060	0.076038
5th	435.041	0.048502	438.816	0.056723	291.753	0.126043
Flutter	4th	$\beta^* = 402$	5th	$\beta^* = 440$	4th	$\beta^* = 227$

As regards to CLD_$[90]_2$, the aeroelastic unstable phenomenon is observed at the fifth mode as differing from the instance of CLD_$[90]_2$ using ISD 110. The flutter boundary of CLD_$[90]_2$ decreases by 191, compared with that of the original base composite panel. CLD_$[90]_2$ shows improved results in free vibration but poor results in aeroelastic analysis when ISD 112 is selected as the viscoelastic layer.

As shown in Fig. 14 and Table 3, in regard to the model with embedded damping layer, the panel flutter occurs at the fourth mode unlike the case using ISD 110, and the flutter boundary (β^*) decreases by 384, compared with that of original base composite panel. The co-cured sandwich model has the worst aeroelastic stability. In free vibration analysis, the selection of viscoelastic material does not significantly affect the natural frequencies and the loss factor. But, in the panel flutter analysis, it affects the aeroelastic stability significantly.

These results show that aeroelastic characteristics as well as dynamic characteristics may improve with the proper damping treatment, but the flutter boundary can change dramatically with the selection of viscoelastic
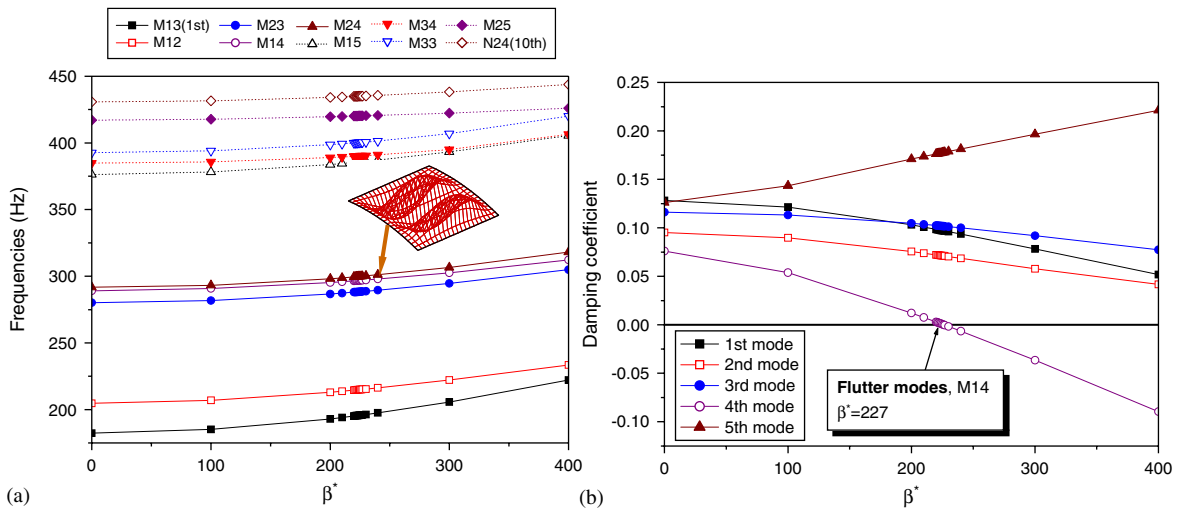
Fig. 14. Flutter history of panel with embedded ISD 112 viscoelastic layer.

material and damping treatments. The optimal design of viscoelastic damping treatment will be a pending problem in view of the improvement of the aeroelastic performance.

4. Conclusion

In this study, the panel flutter of cylindrical hybrid composite panels with viscoelastic layers was investigated by using the finite element method based on the layerwise shell theory considering transverse shear deformations and Kumhaar's modified piston theory. Various damping treatment models such as UCLD, CLD and co-cured models were compared with the original base panel with respect to aeroelastic stability.

Present results show that it is very important to consider the structural damping properties for the accurate estimation of aeroelastic characteristics of cylindrical hybrid composite panels even if the structural damping is very small. In the case where the structural damping was neglected, the results differed by 25% compared with those in case where structural damping was considered. The various damping treatments improved the dynamic stability in previous study, but some cases with surface damping treatments lowered the aeroelastic stability. Therefore, it is necessary to optimally design the damping treatment to improve both dynamic and aeroelastic characteristics of cylindrical hybrid composite panels with viscoelastic layers.

References

[1] D.K. Rao, Frequency and loss factors of sandwich beams under various boundary conditions, *Journal of Mechanical Engineering Science* 20 (1978) 271–282.
[2] M.L. Soni, F.K. Bogner, Finite element vibration analysis of damped structures, *AIAA Journal* 20 (1982) 700–707.
[3] D.A. Saravanos, J.M. Pereira, Dynamic characteristics of specialty composite structures with embedded damping layers, *Journal of Vibration and Acoustics* 117 (1995) 62–69.
[4] K.N. Koo, I. Lee, A refined analysis of vibration and damping for anisotropic laminates in cylindrical bending, *Journal of Sound and Vibration* 184 (1995) 553–566.
[5] K.D. Cho, J.H. Han, I. Lee, Vibration and damping analysis of laminated plates with fully and partially covered damping layers, *Journal of Reinforced Plastics and Composites* 19 (2000) 1176–1200.
[6] D.G. Lee and J.B. Kosmatka, Passively damped vibration of composite plates with zig-zag elements, *41st AIAA/ASME/ASCE/AHS/ASC Structures, Structural Dynamics, and Materials Conference and Exhibit*, AIAA-2000-1473, 2000.
[7] T.C. Ramesh, N. Ganesan, The harmonic response of cylindrical shells with constrained damping treatment, *Journal of Sound and Vibration* 180 (1995) 745–756.
[8] A. Baz, T. Chen, Control of axi-symmetric vibrations of cylindrical shells using active constrained layer damping, *Thin-Walled Structures* 36 (2000) 1–20.

[9] I. Lee, I.K. Oh, W.H. Shin, K.D. Cho, K.N. Koo, Dynamic characteristics of cylindrical composite panels with co-cured and constrained viscoelastic layers, *JSME International Journal, Series C* 45 (2000) 16–25.

[10] E.H. Dowell, Panel flutter: a review of the aeroelastic stability of plates and shells, *AIAA Journal* 8 (1970) 385–399.

[11] D.J. Johns, P.C. Parks, Effect of structural damping on panel flutter, *Aircraft Engineering* 32 (1960) 304–308.

[12] C.H. Ellen, Influence of structural damping on panel flutter, *AIAA Journal* 6 (1968) 2169–2174.

[13] G.A. Oyibo, Unified panel flutter theory with viscous damping effects, *AIAA Journal* 21 (1983) 767–773.

[14] K.N. Koo, W.S. Hwang, Effects of hysteretic and aerodynamic damping on supersonic panel flutter of composite plates, *Journal of Sound and Vibration* 273 (2004) 569–583.

[15] H. Krumhaar, The accuracy of linear piston theory when applied to cylindrical shells, *AIAA Journal* 1 (1963) 1448–1449.

[16] L. Librescu, *Elastostatics and Kinetics of Anisotropic and Heterogeneous Shell-Type Structures*, Noordhoff International Publishing, Leyden, The Netherlands, 1975.

[17] M.H. Bismarck-Nasr, Finite element analysis of aeroelasticity of plates and shells, *Applied Mechanics Review* 45 (1992) 461–482.

[18] R.M.V. Pidaparti, H.T.Y. Yang, Supersonic flutter analysis of composite plates and shells, *AIAA Journal* 31 (1993) 1109–1117.

[19] H. Krause, D. Dinkler, The influence of curvature on supersonic panel flutter, *Proceedings of the 39th AIAA/ASME/ASCE/AHS/ ASC Structures, Structural Dynamics, and Material Conference* AIAA-98-1841, 1998, pp. 1234–1240.

[20] M.N. Bismarck-Nasr, C.A. Bones, Damping effects in nonlinear panel flutter, *AIAA Journal* 38 (2000) 711–713.

[21] I.K. Oh, J.H. Han, I. Lee, Postbuckling and vibration characteristics of piezolaminated composite plate subject to thermo-piezoelectric loads, *Journal of Sound and Vibration* 233 (2000) 19–40.

[22] I.K. Oh, J.H. Han, I. Lee, Thermopiezoelastic snapping of piezolaminated plates using layerwise nonlinear finite elements, *AIAA Journal* 39 (2001) 1188–1198.

[23] I.K. Oh, I. Lee, Thermal snapping and vibration characteristics of cylindrical composite panels using layerwise theory, *Composite Structures* 51 (2001) 49–61.

[24] M. L. Drake, Damping properties of various materials, *Technical Report AFWAL-TR-88-4248*, 1989.